

Inter-Frame Compression for Dynamic Point Cloud Geometry Coding

Anique Akhtar
University of Missouri-Kansas City
Kansas City, MO, USA
aniqueakhtar@mail.umkc.edu

Zhu Li
University of Missouri-Kansas City
Kansas City, MO, USA
zhu.li@ieee.org

Geert Van der Auwera
Qualcomm Technologies Inc.
San Diego, CA, USA
geertv@qti.qualcomm.com

Abstract—Efficient point cloud compression is essential for applications like virtual and mixed reality, autonomous driving, and cultural heritage. In this paper, we propose a deep learning-based inter-frame encoding scheme for dynamic point cloud geometry compression. We propose a lossy geometry compression scheme that predicts the latent representation of the current frame using the previous frame by employing a novel prediction network. Our proposed network utilizes sparse convolutions with hierarchical multiscale 3D feature learning to encode the current frame using the previous frame. We employ *convolution on target coordinates* to map the latent representation of the previous frame to the downsampled coordinates of the current frame to predict the current frame’s feature embedding. Our framework transmits the residual of the predicted features and the actual features by compressing them using a learned probabilistic factorized entropy model. At the receiver, the decoder hierarchically reconstructs the current frame by progressively rescaling the feature embedding. We compared our model to the state-of-the-art Video-based Point Cloud Compression (V-PCC) and Geometry-based Point Cloud Compression (G-PCC) schemes standardized by the Moving Picture Experts Group (MPEG). Our method achieves more than 91% BD-Rate (Bjontegaard Delta Rate) reduction against G-PCC, more than 62% BD-Rate reduction against V-PCC intra-frame encoding mode, and more than 52% BD-Rate savings against V-PCC P-frame-based inter-frame encoding mode using HEVC.

I. INTRODUCTION

A point cloud (PC) is a 3D data representation that is essential for tasks like virtual reality (VR) and mixed reality (MR), autonomous driving, cultural heritage, etc. PCs are a set of points in 3D space, represented by their 3D coordinates (x , y , z) referred to as the *geometry*. Each point may also be associated with multiple *attributes* such as color, normal vectors, and reflectance. Depending on the target application and the PC acquisition methods, the PC can be categorized into point cloud scenes and point cloud objects. Point cloud scenes are typically captured using LiDAR sensors and are often dynamically acquired. Point cloud objects can be further subdivided into static point clouds and dynamic point clouds. A static PC is a single object, whereas a dynamic PC is a time-varying PC where each instance of a dynamic PC is a static PC. Dynamic time-varying PCs are used in AR/VR, volumetric video streaming, and telepresence and can be generated using 3D models, i.e., CGI, or captured from real-world scenarios using various methods such as multiple cameras with depth sensors surrounding the object. These PCs are dense photo-

realistic point clouds that can have a massive amount of points, especially in high precision or large-scale captures (millions of points per frame with up to 60 frames per second (FPS)). Therefore, efficient point cloud compression (PCC) is particularly important to enable practical usage in VR and MR applications.

The Moving Picture Experts Group (MPEG) has approved two PCC standards [1], [2]: Geometry-based Point Cloud Compression (G-PCC) [3] and Video-based Point Cloud Compression (V-PCC) [4]. G-PCC edition 1 includes octree-geometry coding as a generic geometry coding tool and a predictive geometry coding (tree-based) tool which is more targeted toward LiDAR-based point clouds. G-PCC is still developing a triangle meshes or triangle soup (trisoup) based method to approximate the surface of the 3D model. V-PCC on the other hand encodes dynamic point clouds by projecting 3D points onto a 2D plane and then uses video codecs, e.g., High-Efficiency Video Coding (HEVC), to encode each frame over time. MPEG has also proposed common test conditions (CTC) to evaluate test models [5]. For quantitative evaluations, CTC employs point-to-point (D1) and point-to-plane (D2) quality metrics.

Deep learning solutions for image and video encoding have been widely successful [6]. Recently, similar deep learning-based PCC methods [7]–[18] have been shown to provide significant coding gains over traditional methodologies. Point cloud compression represents new challenges due to the unique characteristics of PC. For instance, the unstructured representation of PC data, the sparse nature of the data, as well as the massive number of points per PC, specifically for dense photo-realistic PC, makes it difficult to exploit spatial and temporal correlation. The current deep learning-based PCC solutions are all intra-prediction methods for static point clouds and fail to utilize inter-prediction coding gains by predicting the current frame using previously decoded frames. Following MPEG’s PCC category guidelines, our work seeks to target dense dynamic point clouds used for VR/MR and immersive telecommunications. Sparse dynamically acquired LiDAR-based point clouds are a very different point cloud category that is out of the scope of this work. Ours is the first solution for inter-prediction for lossy point cloud geometry encoding using deep learning and has the following novelties:

- We propose a novel deep learning-based framework for

point cloud geometry inter-frame encoding similar to P-frame encoding in video compression.

- We propose a novel predictor module that learns a feature embedding of the current PC frame from the previous PC frame. The network utilizes hierarchical multiscale feature extractions and employs “*convolution on target coordinates*” to map latent features from the previous frame to the downsampled coordinates of the current frame to learn the current frame’s feature embedding.
- To the best of our knowledge, our method is the first deep learning-based method to outperform V-PCC inter-frame mode across all bitrates. Experimental results show our method achieves more than 91% BD-Rate gains against G-PCC (octree), more than 84% BD-Rate gains against G-PCC (trisoup), more than 34% BD-Rate gains against state-of-the-art deep learning-based point cloud geometry compression method, more than 62% BD-Rate gains against V-PCC intra-frame mode, and more than 52% BD-Rate gains against V-PCC P-frame-based inter-frame mode which uses HEVC.

II. BACKGROUND

Our research is most closely related to three research topics: point cloud geometry compression, deep learning-based video inter-frame coding, and deep learning-based point cloud compression.

Prior non-deep learning-based point cloud geometry compression mostly includes *octree-based*, *triangle mesh-based*, and *3D-to-2D projection-based* methodologies. **Octree-based methods** are the most widely used point cloud encoding methods [19]–[21]. Octree provides an efficient way to partition the 3D space to represent point clouds and is especially suitable for lossless coding. In these methods, the volumetric point cloud is recursively divided into octree decomposition until it reaches the leaf nodes. Then the occupancy of these nodes can be compressed through an entropy context modeling conditioned on neighboring and parent nodes. Thanou et al. [22], [23] implemented octree-based encoding for time-varying point clouds that can predict graph-encoded octree structures between adjacent frames. MPEG’s G-PCC standard [1] also employs an octree-based compression method known as *octree geometry codec* and is specifically devoted to sparse point clouds. G-PCC encoding can further be complemented by triangle meshes (a.k.a., triangle soups) which are locally generated together with the octree to terminate the octree decomposition prematurely. This helps reconstruct object surfaces with finer spatial details and is known as the *trisoup geometry codec* [24].

3D-to-2D projection-based methods. Traditional 2D image and video coding have demonstrated outstanding efficiency and have been widely used in standards which have motivated works to project 3D objects to multiple 2D planes and leverage popular image and video codecs for compact representation. MPEG’s V-PCC [2] standard is one such 3D-to-2D projection-based solution that is specifically designed for dense, as well as, dynamic PCs. The V-PCC standard projects the points and

the corresponding attributes onto planes and then uses a state-of-the-art video codec, such as HEVC, to encode point clouds. V-PCC has both intra-frame coding as well as inter-frame coding where the previously decoded frames are employed to encode the next frames. We have also had some other works specifically for **dynamic point cloud compression** [25]–[27]. However, their results are still lacking and not comparable to V-PCC.

Deep learning-based models for image and video encoding can learn an optimal non-linear transform from data along with the probabilities required for entropy coding the latent representation into a bitstream in an end-to-end fashion. For image compression, autoencoders [28] were initially adopted and the best results were achieved by employing variational autoencoders with side information transmission and applying an autoregressive model [29]. Deep learning solutions for video compression methods usually employ 3D autoencoders, frame interpolation, and/or motion compensation via optical flow. 3D autoencoders are an extension of deep learned image compression. Frame interpolation methods use neural networks to temporally interpolate between frames in a video and then encode the residuals [30]. Motion compensation via optical flow is based on estimating and compressing optical flow which is applied with bilinear warping to a previously decoded frame to obtain a prediction of the frame currently being encoded [31]. Current deep learning-based PCC takes inspiration from the deep learning-based image compression methods but so far has not been able to implement inter-frame prediction models commonly used in video encoding. Our work is the first method that takes inspiration from the frame interpolation-based methods in video encoding to perform inter-frame encoding for dynamic point clouds.

Deep learning-based Geometry PCC can be broadly categorized into: *voxelization-based methods*, *octree-based methods*, *point-based methods*, and *sparse tensors-based methods*. **Voxelization-based methods** were employed in the earlier approaches, including Quach et al. [7], Wang et al. [8], Guarda et al. [9] and Quach et al. [10]. These methods voxelizes the PC and then divide it into smaller blocks typically of $64 \times 64 \times 64$ voxels. Then 3D convolutions are applied using autoencoder architectures to compress these blocks into latent representations. These methods usually employ a focal loss or a weighted binary cross-entropy loss to train their model. However, these methods also have to process empty voxels which are usually the majority of the voxels and are, therefore, computational and memory inefficient.

Octree-based methods employ octree representation to encode the PCs leading to better consumption of storage and computation. These methods employ entropy context modeling to predict each node’s occupancy probability conditioned on its neighboring and parent nodes. MuSCLE [11] and OctSqueeze [12] employ Multi-Layer Perceptrons (MLPs) to exploit the dependency between parent and child nodes. VoxelContextNet [13] employs both neighbors and parents as well as voxelized neighborhood points as context for probability approximation. Recently, OctAttention [14] has been introduced

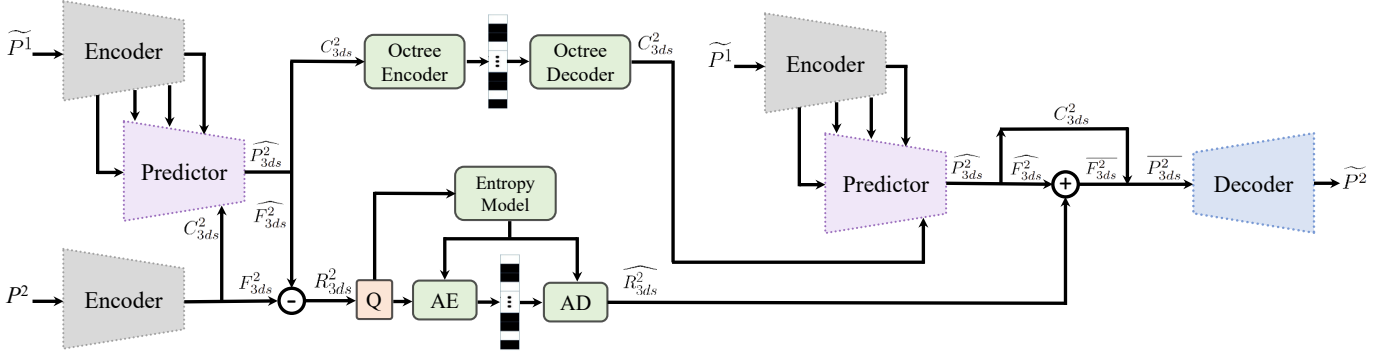


Fig. 1. System Model. The previously decoded frame \tilde{P}^1 is employed to encode a feature embedding of the current frame P^2 . Multiscale features from \tilde{P}^1 and three-times downsampled coordinates C^2_{3ds} from P^2 are passed to the Predictor network to learn a feature embedding $\tilde{P}^2_{3ds} = \{C^2_{3ds}, \tilde{F}^2_{3ds}\}$. Current frame's three-times downsampled coordinates C^2_{3ds} are transmitted in a lossless manner using octree encoder. The predicted downsampled features \tilde{F}^2_{3ds} and the original downsampled features F^2_{3ds} are subtracted to obtain the residual features R^2_{3ds} . The residual is transmitted in a lossy manner using a learned entropy model. The same Encoder and Predictor module is used throughout the system.

that increases the receptive field of the context model by employing a large-scale transformer-based context attention module to estimate the probability of occupancy code. All of these methods encode the point cloud in a lossless manner and show promising results, particularly on sparse LiDAR-based point clouds.

Point-based methods directly process raw point cloud data without changing their representation or voxelizing them. They typically employ PointNet [32] or PointNet++ [33] type architectures that process raw point clouds using point-wise fully connected layers. These methods are typically patch-based methods that employ farthest point sampling to subsample and a knn search to find per point feature embedding to build an MLP-based autoencoder. However as seen in some of these works [15], [16], [34], the coding efficiency of such point-wise models is still relatively low and fails to generalize to large-scale dense point clouds. Furthermore, these methods require a lot of pre and post-processing making the encoding process computationally inefficient.

Recent **sparse convolution-based methods** [17], [18] have shown really good results especially for denser photo-realistic point clouds. Sparse convolutions exploit the inherent sparsity of point cloud data for complexity reduction allowing for very large point clouds to be processed by a deeper sparse convolutional network. This allows the network to better capture the characteristics of sparse and unstructured points and better extraction of local and global 3D geometric features. However, all of these works employ intra-frame encoding for static point clouds. We employ sparse convolution-based autoencoder architecture similar to [17] and design a sparse convolutional inter-frame prediction module that encodes the next PC frame using the previously decoded PC frame similar to P-frame prediction in video encoding.

III. PROPOSED METHOD

The proposed lossy inter-frame point cloud geometry compression framework is illustrated in Fig. 1. We employ sparse tensors and sparse convolutions to decrease the computational

complexity of the network so it can process two PC frames. The solution is inspired by the PCGCv2 [17] multiscale point cloud geometry compression (PCGC) work. PCGCv2 is an intra-frame point cloud compression scheme suitable for static point clouds. Our inter-frame prediction scheme uses an encoder and decoder network similar to PCGCv2 along with a novel prediction network to predict a feature embedding for the current PC frame from the previous PC frame. We calculate the residual between the predicted and ground truth features and transmit the residuals along with the three-times downsampled coordinates. The three-times downsampled coordinates are losslessly encoded by an octree encoder using G-PCC [3], whereas the residual features are encoded in a lossy manner using factorized entropy model to predict the probability distribution for arithmetic coding. It should be noted that in our system, the encoder and prediction network is present both at the transmitter as well as the receiver. We train the networks with joint reconstruction and bit-rate loss to optimize rate distortion. We provide a detailed description of all our modules in subsequent discussions.

A. Problem Formulation and Preprocessing

We adopt sparse convolutions for low-complexity tensor processing and build our system using Minkowski Engine [35]. Each point cloud frame is converted into a sparse tensor P . Each point cloud tensor $P = \{C_n, F_n\}_n$ is represented by a set of coordinates $C = \{(x_n, y_n, z_n)\}_n$ and their associated features $F = \{f(x_n, y_n, z_n)\}_n$. Only the occupied coordinates are kept in a sparse tensor. To initialize the input point cloud as geometry only, we assign feature $f(x, y, z) = 1$ to each occupied coordinate. Given a dynamic point cloud with multiple frames, P^i , our goal is to convert them into a latent representation with the smallest possible bitrate. We use P-frame encoding where the current frame is encoded using the prediction from the previous frame. We denote the Encoder network as E , and the Decoder network as D .

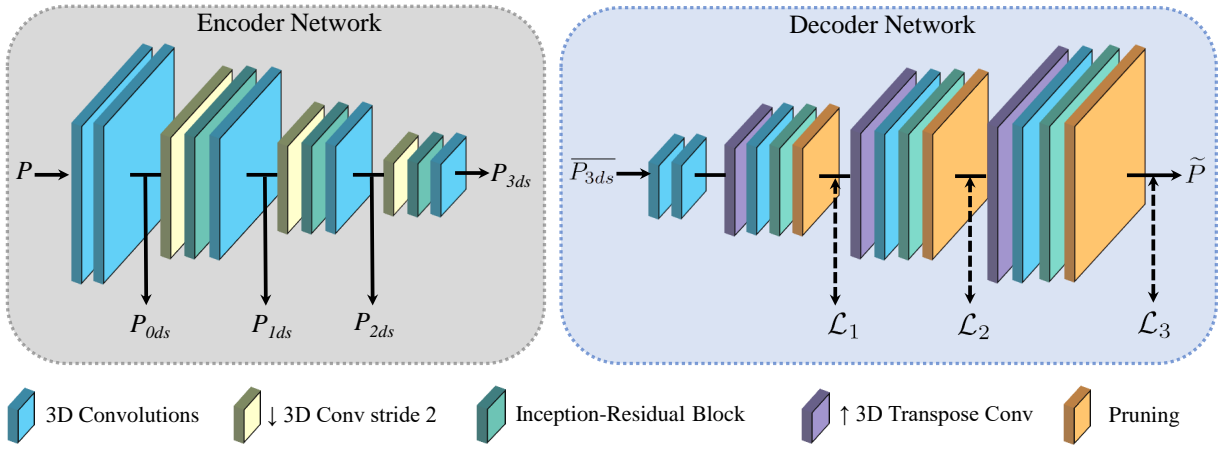


Fig. 2. Encoder and Decoder Network. The encoder network takes the original point cloud sparse tensor P , and creates sparse features at four different scales: P_{0ds} , P_{1ds} , P_{2ds} , and P_{3ds} . Where $3ds$ denotes three-times downsampled sparse tensor. The decoder network takes the three-times downsampled sparse tensor and hierarchically reconstructs the original point cloud by progressively rescaling. The decoder upsamples the sparse tensor followed by a pruning layer to prune false voxels.

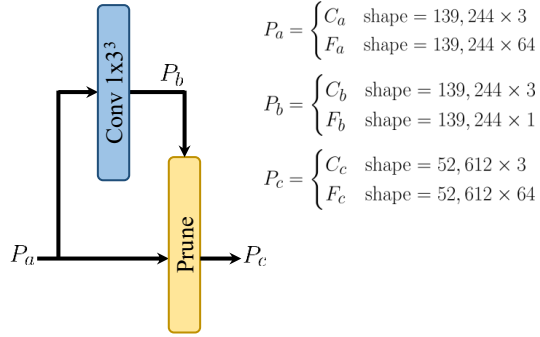


Fig. 3. Example of pruning layer with input sparse tensor P_a and output sparse tensor P_c . Binary classification is applied to P_b to chose the top voxels and prune false voxels from P_a to obtain P_c .

B. Encoder, Decoder, and Pruning

Our encoder and decoder network is shown in Fig. 2. We utilize the Inception-Residual Block (IRB) from PCGCv2 [17] for feature extraction in all our networks. We employ a multi-scale re-sampling with downscaling at the encoder and upscaling at the decoder. This helps exploit the sparsity of the PC while encoding 3D geometric structural variations into feature attributes of the latent representation. The encoder helps us obtain PC tensors at four different scales capturing multiscale features at different level of details: $P_{0ds}, P_{1ds}, P_{2ds}, P_{3ds} = E(P)$. Where P_{ids} represents a sparse tensor P that has been downsampled i times. The decoder receives a three-times downsampled PC tensor and upsamples it hierarchically to reconstruct the original PC tensor by employing a different reconstruction loss at each scale: $\tilde{P} = D(P_{3ds})$. Decoder employs transpose convolution to upsample the PC tensor. Encoder and decoder architecture can on their own be used for intra-frame PC compression, the details of which are available from PCGCv2 [17].

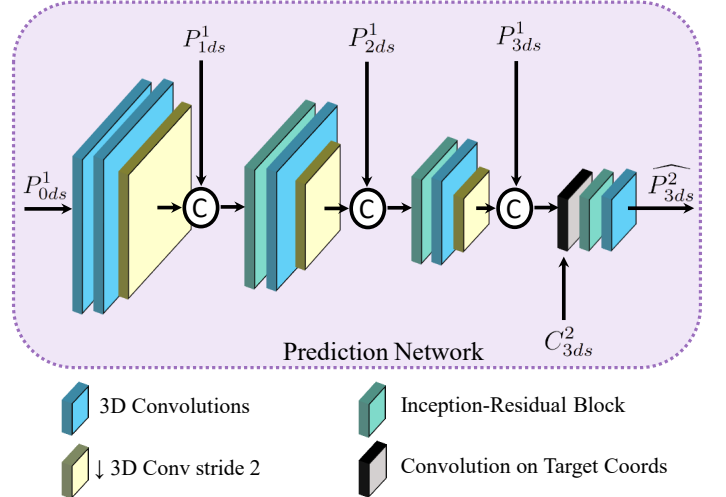


Fig. 4. Prediction network. Takes in four multiscale features from previous frame and the three-times downsampled coordinates of the current frame (C_{3ds}^2) to learn current frame's feature embedding \hat{P}_{3ds}^2 .

The geometry at the decoder is reconstructed by employing a pruning layer to prune false voxels and extract true occupied voxels using binary classification after each upscaling. One example of a pruning layer is shown in Fig. 3. In this example, the input sparse tensor P_a has coordinates C_a of shape $139,244 \times 3$ and their corresponding features of shape $139,244 \times 64$. We pass P_a through a convolution of channel size 1 to obtain sparse tensor P_b with features F_b of shape $139,244 \times 1$. From F_b we select the topk features (in this example $k = 52,612$) and their corresponding coordinates using binary classification. The false coordinates and their corresponding features are then pruned from P_a to obtain P_c . During training, the binary voxel classification loss is applied to P_b to learn the proper point cloud reconstruction.

C. Overall System Model

The overall working of the proposed method is shown in Fig. 1. In our work, we denote the current PC frame as P^2 while the previously decoded PC frame is denoted by \tilde{P}^1 . The same encoder and prediction module are used throughout the system to decrease the number of parameters. Previously decoded frame \tilde{P}^1 is passed through the encoder to obtain multiscale features $P_{0ds}^1, P_{1ds}^1, P_{2ds}^1, P_{3ds}^1$. The current frame P^2 is also passed through the encoder to obtain three-times downsampled tensor containing coordinates and features: $P_{3ds}^2 = \{C_{3ds}^2, F_{3ds}^2\}$. Current frame's three-times downsampled coordinates and the multiscale features from the previous frame are passed to the prediction network to obtain current frame's predicted three-times downsampled tensor $\hat{P}_{3ds}^2 = \{\hat{C}_{3ds}^2, \hat{F}_{3ds}^2\}$. The predicted downsampled features \hat{F}_{3ds}^2 and the original downsampled features F_{3ds}^2 are subtracted to obtain the residual features R_{3ds}^2 . The residual is transmitted in a lossy manner using a factorized entropy model [28]. The current frame's three-times downsampled coordinates C_{3ds}^2 are transmitted in a lossless manner using an octree encoder like G-PCC [3]. Three-times downsampled coordinates C_{3ds}^2 is much smaller than the original geometry (e.g. for the 8iVFB dataset, the C_{3ds}^2 is about 16 times smaller than C^2). At the receiver, the previously decoded frame \tilde{P}^1 and the three-times downsampled coordinates C_{3ds}^2 are used to predict \hat{P}_{3ds}^2 . The residual \hat{R}_{3ds}^2 is added with \hat{P}_{3ds}^2 to obtain the current frame's three-times downsampled tensor representation \hat{P}_{3ds}^2 . The decoder progressively rescales \hat{P}_{3ds}^2 to obtain the current decoded frame \tilde{P}^2 .

D. Prediction Network

We propose a novel deep learning-based inter-frame prediction network that can predict the latent representation of the current frame from the previously reconstructed frame as shown in Fig. 4. This way the network performs motion estimation between consecutive frames to measure the current frame's feature embedding. The multiscale features from the previous frame, $P_{0ds}^1, P_{1ds}^1, P_{2ds}^1, P_{3ds}^1$, and the three downsampled coordinates from the current frame, C_{3ds}^2 , are fed to the prediction network to obtain current frame's predicted three-times downsampled tensor $\hat{P}_{3ds}^2 = \{\hat{C}_{3ds}^2, \hat{F}_{3ds}^2\}$. The prediction network downscales the input three times while concatenating it with the corresponding scale features. Finally we employ a **convolution on target coordinates** to obtain features for \hat{P}_{3ds}^2 . *Convolution on target coordinates* help us translate the latent features from the downsampled coordinates of P^1 , i.e., C_{3ds}^1 to the downsampled coordinates of P^2 , i.e., C_{3ds}^2 . *Convolution on target coordinates* can be viewed as a convolution with arbitrary input and output coordinates where the features from input coordinates get convolved with the convolutional kernel and the output is only retained at the output coordinates. An example of *Convolution on target coordinates* is shown in Fig. 5. During *convolution on target coordinates*, the features are mapped from the input coordinates C_{3ds}^1 to the output coordinates C_{3ds}^2 after applying sparse convolution.

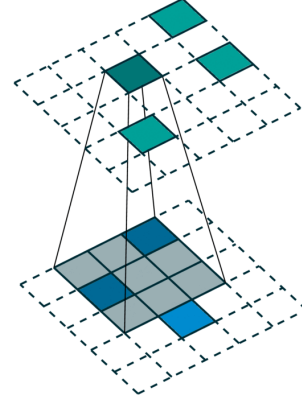


Fig. 5. Example of convolution on target coordinates in 2D. Where the blue are the input coordinates and the green are the output coordinates. (figure taken from [35]).

We use a kernel size of $3 \times 3 \times 3$ for the *convolution on target coordinates*.

E. Training

During training, we optimize the Lagrangian loss, i.e.,

$$J_{loss} = R + \lambda D \quad (1)$$

Where R is the compressed bit rate and D is the distortion loss. We employ binary cross-entropy loss for voxel occupancy classification as the distortion loss at the decoder. We employ three binary cross-entropy losses at three different scales such that the total distortion loss is:

$$D = \mathcal{L}_1(\tilde{P}_{2ds}, P_{2ds}) + \mathcal{L}_2(\tilde{P}_{1ds}, P_{1ds}) + \mathcal{L}_3(\tilde{P}, P) \quad (2)$$

Where the ground-truth P_{2ds} and P_{1ds} are obtained by voxel or quantization-based downsampling of the original point cloud P .

The three downsampled coordinates C_{3ds}^2 are transmitted losslessly using Octree encoder in G-PCC [3] and consumes a very small amount of bits (i.e., around 0.024 bpp for 8iVFB dataset). We subtract the three downsampled predicted features \hat{F}_{3ds}^2 from the original three downsampled features F_{3ds}^2 to obtain the residual features R_{3ds}^2 . The residual features are quantized during inference, while during training, uniform noise is used to approximate the quantization [28]. Quantized residual features are encoded by an arithmetic encoder where a fully factorized probabilistic entropy model [29] is used to learn the probability distribution of each feature where the bitrate (R) is lower bounded by its information entropy.

IV. EXPERIMENTAL RESULTS

A. Dataset and Training

We used a total of eight different sequences for dynamic point cloud datasets: *longdress*, *loot*, *redandblack*, and *soldier* sequences from JPEG Plenos 8i Voxelized Full Bodies dataset (8iVFB v2) [36], *queen* sequence from Technicolor (<https://www.technicolor.com/fr>), and *basketball*, *exercise*, and

TABLE I
BD-RATE GAINS AGAINST THE STATE-OF-THE-ART METHODS USING D1 DISTORTION MEASUREMENTS.

	G-PCC (octree)	G-PCC (trisoup)	PCGCv2 [17]	V-PCC intra	V-PCC inter
basketball	-92.01	-87.80	-32.45	-60.46	-48.82
exercise	-91.70	-87.02	-35.44	-62.08	-48.30
model	-89.86	-83.24	-33.69	-61.93	-51.80
redandblack	-91.42	-81.25	-28.31	-59.33	-55.58
soldier	-92.75	-82.61	-40.16	-66.51	-43.60
Average	-91.68	-84.41	-34.08	-62.69	-52.44

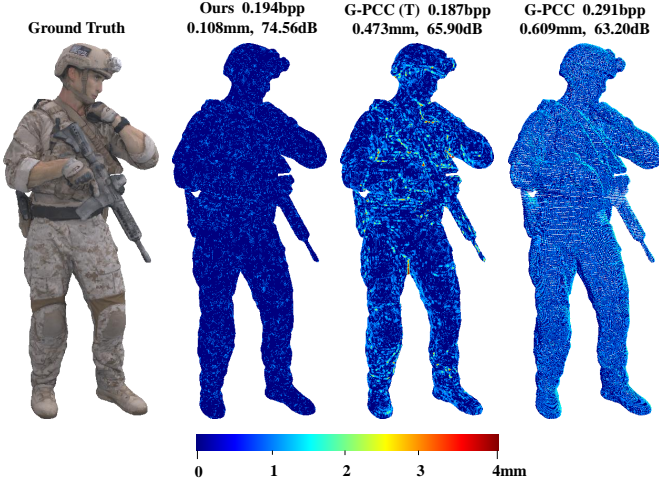


Fig. 6. Qualitative visual comparison of sequence “soldier” for different methods. The color error map describes the point-to-point distortion measured in mm, and the numbers above represent the bitrate, mean error measured in mm, and D1 PSNR.

model sequences from MPEG’s **Owl** Dynamic Human Textured Mesh Sequence Dataset [37]. We converted all the dynamic datasets to a voxel depth of 10 bits. The 8iVFB and queen datasets have about 300 frames whereas Owl dataset has 64 frames.

We train the proposed inter-frame encoding method in an end-to-end manner using dynamic point cloud datasets. During training, *longdress*, *loot* and *queen* sequences were used; while sequences *redandblack*, *soldier*, *basketball*, *exercise*, and *model* were used during testing. To decrease computational complexity during training, we divide the PC frames into smaller chunks by applying the same kd-tree partition on two consecutive frames. During inference time we used whole point clouds. We use seven different λ values to cover a wide range of bit rates.

B. Performance Evaluation.

For a fair comparison, we closely follow MPEG’s common test conditions (CTC) [5]. We compare our method to the state-of-the-art deep learning intra-frame encoding PCGCv2 [17], MPEG’s G-PCC (octree as well as trisoup) [3] methods, as well as MPEG’s video-based V-PCC method (inter and intra-frame encoding) [4]. We utilize G-PCC’s latest reference implementation TMC13-v14 and for V-PCC the latest implementation TMC2-v17 is employed that uses HEVC video

codec. We employ V-PCC inter-frame low-delay setting which involves P-frame encoding for a fair comparison to our P-frame encoding scheme. We employ MPEG’s point-to-point distance (D1) mean squared error (MSE) based Peak Signal-to-Noise Ratio (PSNR) as our evaluation metrics. *Bits per point* (bpp) is used to measure the compression ratio. We plot rate-distortion curves and calculate the BD-Rate (Bjontegaard Delta Rate) [38] gains over different methods.

Table I shows the BD-Rate gains of the proposed method over the state-of-the-art. The lower the BD-Rate value, the more the improvement is. Our method achieves significant gains compared to G-PCC with an average of 91.68% BD-Rate gains against G-PCC (octree), 84.41% BD-Rate improvement over G-PCC (trisoup). Compared to the deep learning-based model PCGCv2, we achieve a 34.08% BD-Rate improvement. Compared to the V-PCC, we achieve a 62.69% BD-Rate improvement over intra-frame encoding mode and 52.44% BD-Rate improvement over inter-frame encoding mode. To the best of our knowledge, our method is the first deep learning-based method to outperform V-PCC inter-frame mode across all rates for dense photo-realistic point clouds.

The rate-distortion curves for each test sequence and their average is plotted in Fig. 7. Fig. 8 shows the zoomed-in version of Fig. 7. As can be seen, our method performs considerably better than G-PCC (octree) and G-PCC (trisoup) and has significant coding gains compared with the deep learning-based model PCGCv2. It should be noted that compared with PCGCv2, our method performs much better at higher PSNR and still performs better than PCGCv2 at lower PSNRs. This is because both the proposed method and PCGCv2 transmit the three downsampled coordinates in a lossless manner and their corresponding features in a lossy manner. However, at lower PSNRs, most of the bits are consumed by coordinates (i.e., around 0.024 bpp) which constitutes the majority of the bitrate. At higher PSNR values most of the bitrates are due to features. Our inter-frame prediction network transmits only the residual of the features and, hence, can significantly decrease the feature bits transmitted leading to much higher gains at higher PSNR and bitrates.

Compared with V-PCC, we can see that we achieve a much higher PSNR for the same bitrate for all of the sequences and bitrates. As expected, the V-PCC inter-frame encoding mode performs better than V-PCC intra-frame encoding mode. The sequences that have the most movement (i.e., *redandblack*) the V-PCC inter and V-PCC intra modes perform pretty similarly whereas the sequence with the least amount of movement (i.e.,

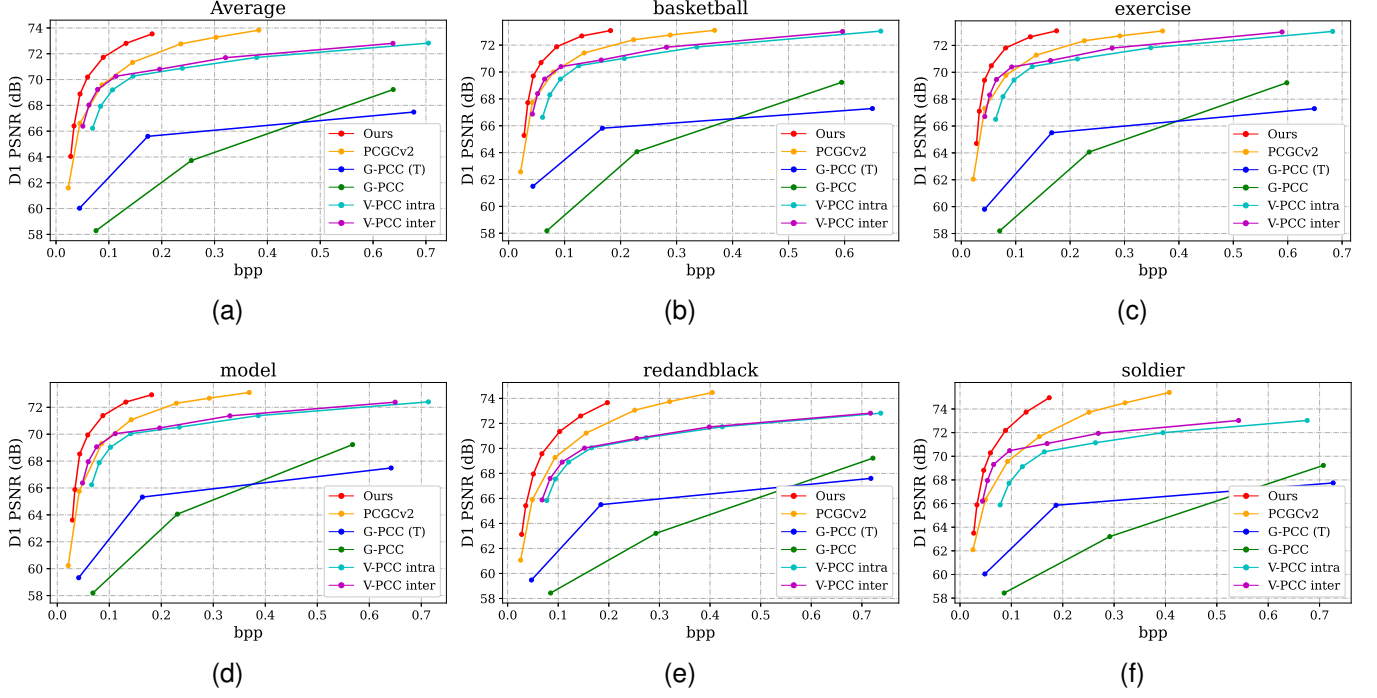


Fig. 7. Rate-distortion curves comparison with the state-of-the-arts plotted for five different sequences and their average.

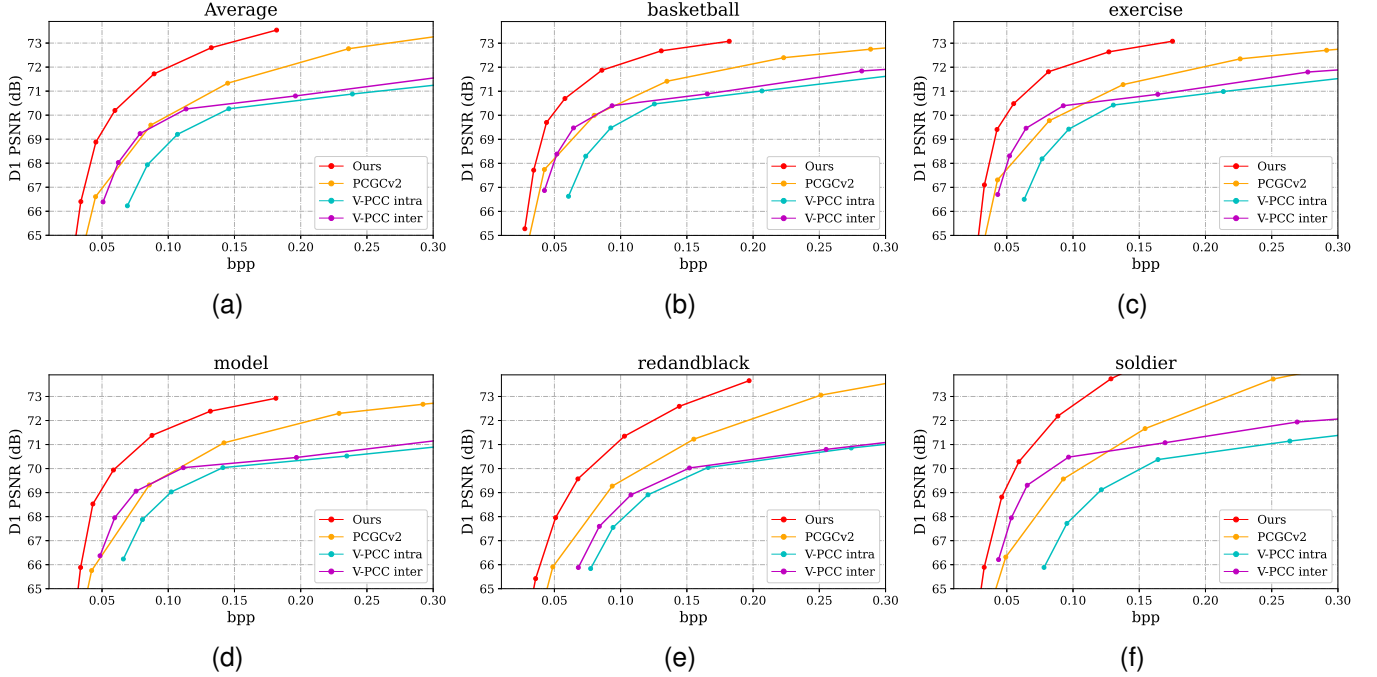


Fig. 8. Zoomed-in version of Fig. 7.

soldier) the V-PCC inter-frame encoding method performed much better than V-PCC intra-frame encoding method. We can see a similar pattern between our proposed inter-frame method and PCGCv2 which is an intra-frame method. We see that our proposed inter-frame method has the most improvement over

PCGCv2 on soldier sequence and the least improvement over PCGCv2 on redandblack sequence. Our Prediction module maps the features extracted from the previous frame to the coordinates extracted from the current frame. In this way, when the motion between adjacent frames is small, the performance

TABLE II
AVERAGE RUNTIME OF DIFFERENT METHODS USING 8iVFB v2 PCs.

	G-PCC (O)	G-PCC (T)	PCGCv2 [17]	Ours
Enc (s)	1.13	6.15	0.258	0.364
Dec (s)	0.44	5.01	0.537	0.714

is significantly improved.

Qualitative comparison with G-PCC and our proposed method is presented in Fig. 6, using point clouds colored by reconstruction error.

C. Runtime Comparison

We compare the runtime of different methods in Table II. We use an Intel Core i9-11900F CPU and an Nvidia GeForce GTX 3090 GPU. G-PCC runtime is computed for the highest bitrate on a CPU. While both PCGCv2 and Our method utilize the GPU. Due to the diversity in platforms, e.g., CPU vs. GPU, Python vs. C/C++, etc, the running time comparison only serves as the intuitive reference to have a general idea about the computational complexity. As can be seen, our method experiences a slight increase in runtime due to processing two PC frames at a time. However, the increased complexity is still minimal given that our network is an inter-frame prediction scheme. PCGCv2 has about 778 thousand parameters, whereas, the proposed method has about 2,033 thousand parameters which is still a relatively small network. The runtime complexity can be optimized by migrating to a C++ implementation and simplifying the framework.

D. Ablation Study: Block Size

Even though in our evaluations, we have used the full point cloud during inference. We wanted to see the effects on PSNR and bitrate of dividing the point cloud into smaller blocks for encoding. The purpose is to demonstrate that if needed, a large point cloud can be partitioned into blocks for processing. During the encoding, we save the *coordinate bitstream*, *feature bitstream*, *number of points*, and the *entropy model header information* into four different files. Overall bitrate is decided by the collective size of these files. Once we divide the point cloud into blocks, each block would be encoded separately into four different files so we should expect to see a higher overhead involved. kd-tree partitioning is employed to divide each point cloud into multiple blocks and encoded the blocks independently. The results of this experiment on *soldier* sequence are shown in Table III. We notice that partitioning the point cloud into smaller blocks decreases the PSNR slightly. However, the difference is minimal. We also notice that the bitrate increases a bit but that could possibly be from the overhead of saving the information in lots of files (e.g. for 8 # of blocks, we have a total of 24 files encoded, whereas, for 1 block, we have a total of 4 files encoded). It is possible to merge these files into a single file to decrease the overhead. However, that is out of the scope of the current work.

TABLE III
PARTITIONING THE POINT CLOUD INTO SMALLER NUMBER OF BLOCKS.
TESTED ON SOLDIER SEQUENCE

# of blocks	PSNR	bpp
1	74.56	0.1944
2	74.52	0.1987
4	74.48	0.2055
8	74.35	0.2158

V. CONCLUSION

In this work, we propose a deep learning-based inter-frame compression scheme for dynamic point clouds that encodes the current frame using the previously decoded previous frame. We employ an encoder to obtain multi-scale features and a decoder to hierarchically reconstruct the point cloud by progressive scaling. We introduce a novel prediction network module that predicts the latent representation of the current frame by mapping the latent features of the previous frame to the downsampled coordinates of the current frame using *convolution on target coordinates*. We encode and transmit the residual of the predicted features and the actual features. We employ sparse convolutions to reduce the space and time complexity which allows our network to process two consecutive point cloud frames. Experimental results show more than 91% BD-Rate gains over the state-of-the-art MPEG G-PCC (octree), more than 84% BD-Rate gains over G-PCC (trisooup), more than 34% BD-Rate gains over intra-frame network PCGCv2, more than 62% BD-Rate improvement over MPEG V-PCC intra-frame encoding mode, and more than 52% BD-Rate improvement over MPEG V-PCC inter-frame encoding mode.

REFERENCES

- [1] S. Schwarz, M. Preda, V. Baroncini, M. Budagavi, P. Cesar, P. A. Chou, R. A. Cohen, M. Krivokuća, S. Lasserre, Z. Li *et al.*, “Emerging MPEG standards for point cloud compression,” *IEEE Journal on Emerging and Selected Topics in Circuits and Systems*, vol. 9, no. 1, pp. 133–148, 2018.
- [2] D. Graziosi, O. Nakagami, S. Kuma, A. Zaghetto, T. Suzuki, and A. Tabatabai, “An overview of ongoing point cloud compression standardization activities: Video-based (v-pcc) and geometry-based (g-pcc),” *APSIPA Transactions on Signal and Information Processing*, vol. 9, 2020.
- [3] “MPEG-PCC-TMC13: Geometry Based Point Cloud Compression G-PCC,” 2021. [Online]. Available: <https://github.com/MPEGGroup/mpeg-pcc-tmc13>
- [4] “MPEG-PCC-TMC2: Video Based Point Cloud Compression VPCC,” 2022. [Online]. Available: <https://github.com/MPEGGroup/mpeg-pcc-tmc2>
- [5] S. Schwarz, G. Martin-Cocher, D. Flynn, and M. Budagavi, “Common test conditions for point cloud compression,” *Document ISO/IEC JTC1/SC29/WG11 w17766, Ljubljana, Slovenia*, 2018.
- [6] D. Liu, Y. Li, J. Lin, H. Li, and F. Wu, “Deep learning-based video coding: A review and a case study,” *ACM Computing Surveys (CSUR)*, vol. 53, no. 1, pp. 1–35, 2020.
- [7] M. Quach, G. Valenzise, and F. Dufaux, “Learning convolutional transforms for lossy point cloud geometry compression,” in *2019 IEEE International Conference on Image Processing (ICIP)*. IEEE, 2019, pp. 4320–4324.
- [8] J. Wang, H. Zhu, H. Liu, and Z. Ma, “Lossy point cloud geometry compression via end-to-end learning,” *IEEE Transactions on Circuits and Systems for Video Technology*, 2021.

- [9] A. F. Guarda, N. M. Rodrigues, and F. Pereira, "Adaptive deep learning-based point cloud geometry coding," *IEEE Journal of Selected Topics in Signal Processing*, vol. 15, no. 2, pp. 415–430, 2020.
- [10] M. Quach, G. Valenzise, and F. Dufaux, "Improved deep point cloud geometry compression," in *2020 IEEE 22nd International Workshop on Multimedia Signal Processing (MMSP)*. IEEE, 2020, pp. 1–6.
- [11] S. Biswas, J. Liu, K. Wong, S. Wang, and R. Urtasun, "MuSCLE: Multi Sweep Compression of LiDAR using Deep Entropy Models," *Advances in Neural Information Processing Systems*, vol. 33, pp. 22 170–22 181, 2020.
- [12] L. Huang, S. Wang, K. Wong, J. Liu, and R. Urtasun, "Octsqueeze: Octree-structured entropy model for LiDAR compression," in *Proceedings of the IEEE/CVF Conference on Computer Vision and Pattern Recognition*, 2020, pp. 1313–1323.
- [13] Z. Que, G. Lu, and D. Xu, "VoxelContext-Net: An Octree based Framework for Point Cloud Compression," in *Proceedings of the IEEE/CVF Conference on Computer Vision and Pattern Recognition*, 2021, pp. 6042–6051.
- [14] C. Fu, G. Li, R. Song, W. Gao, and S. Liu, "Octattention: Octree-based large-scale contexts model for point cloud compression," *arXiv preprint arXiv:2202.06028*, 2022.
- [15] L. Gao, T. Fan, J. Wan, Y. Xu, J. Sun, and Z. Ma, "Point cloud geometry compression via neural graph sampling," in *2021 IEEE International Conference on Image Processing (ICIP)*. IEEE, 2021, pp. 3373–3377.
- [16] K. You and P. Gao, "Patch-based deep autoencoder for point cloud geometry compression," in *ACM Multimedia Asia*, 2021, pp. 1–7.
- [17] J. Wang, D. Ding, Z. Li, and Z. Ma, "Multiscale Point Cloud Geometry Compression," in *2021 Data Compression Conference (DCC)*. IEEE, 2021, pp. 73–82.
- [18] J. Wang, D. Ding, Z. Li, X. Feng, C. Cao, and Z. Ma, "Sparse Tensor-based Multiscale Representation for Point Cloud Geometry Compression," *arXiv preprint arXiv:2111.10633*, 2021.
- [19] R. Mekuria, K. Blom, and P. Cesar, "Design, implementation, and evaluation of a point cloud codec for tele-immersive video," *IEEE Transactions on Circuits and Systems for Video Technology*, vol. 27, no. 4, pp. 828–842, 2016.
- [20] D. C. Garcia and R. L. de Queiroz, "Intra-frame context-based octree coding for point-cloud geometry," in *2018 25th IEEE International Conference on Image Processing (ICIP)*. IEEE, 2018, pp. 1807–1811.
- [21] M. Krivokuća, P. A. Chou, and M. Koroteev, "A volumetric approach to point cloud compression—part ii: Geometry compression," *IEEE Transactions on Image Processing*, vol. 29, pp. 2217–2229, 2019.
- [22] D. Thanou, P. A. Chou, and P. Frossard, "Graph-based compression of dynamic 3d point cloud sequences," *IEEE Transactions on Image Processing*, vol. 25, no. 4, pp. 1765–1778, 2016.
- [23] —, "Graph-based motion estimation and compensation for dynamic 3d point cloud compression," in *2015 IEEE International Conference on Image Processing (ICIP)*. IEEE, 2015, pp. 3235–3239.
- [24] C. Cao, M. Preda, V. Zakharchenko, E. S. Jang, and T. Zaharia, "Compression of sparse and dense dynamic point clouds - methods and standards," *Proceedings of the IEEE*, vol. 109, no. 9, pp. 1537–1558, 2021.
- [25] D. C. Garcia, T. A. Fonseca, R. U. Ferreira, and R. L. de Queiroz, "Geometry coding for dynamic voxelized point clouds using octrees and multiple contexts," *IEEE Transactions on Image Processing*, vol. 29, pp. 313–322, 2019.
- [26] P. Gomes, "Graph-based network for dynamic point cloud prediction," in *Proceedings of the 12th ACM Multimedia Systems Conference*, 2021, pp. 393–397.
- [27] R. L. De Queiroz and P. A. Chou, "Motion-compensated compression of dynamic voxelized point clouds," *IEEE Transactions on Image Processing*, vol. 26, no. 8, pp. 3886–3895, 2017.
- [28] J. Ballé, V. Laparra, and E. P. Simoncelli, "End-to-end optimized image compression," *arXiv preprint arXiv:1611.01704*, 2016.
- [29] J. Ballé, D. Minnen, S. Singh, S. J. Hwang, and N. Johnston, "Variational image compression with a scale hyperprior," *arXiv preprint arXiv:1802.01436*, 2018.
- [30] A. Djelouah, J. Campos, S. Schaub-Meyer, and C. Schroers, "Neural inter-frame compression for video coding," in *Proceedings of the IEEE/CVF International Conference on Computer Vision*, 2019, pp. 6421–6429.
- [31] G. Lu, W. Ouyang, D. Xu, X. Zhang, C. Cai, and Z. Gao, "DVC: An end-to-end deep video compression framework," in *Proceedings of the IEEE/CVF Conference on Computer Vision and Pattern Recognition*, 2019, pp. 11 006–11 015.
- [32] C. R. Qi, H. Su, K. Mo, and L. J. Guibas, "PointNet: Deep Learning on Point Sets for 3D Classification and Segmentation," in *Proceedings of the IEEE conference on computer vision and pattern recognition*, 2017, pp. 652–660.
- [33] C. R. Qi, L. Yi, H. Su, and L. J. Guibas, "PointNet++: Deep hierarchical feature learning on point sets in a metric space," *Advances in neural information processing systems*, vol. 30, 2017.
- [34] T. Huang and Y. Liu, "3D point cloud geometry compression on deep learning," in *Proceedings of the 27th ACM international conference on multimedia*, 2019, pp. 890–898.
- [35] C. Choy, J. Gwak, and S. Savarese, "4D Spatio-Temporal ConvNets: Minkowski Convolutional Neural Networks," in *Proceedings of the IEEE Conference on Computer Vision and Pattern Recognition*, 2019, pp. 3075–3084.
- [36] E. d'Eon, B. Harrison, T. Myers, and P. A. Chou, "8i Voxelized Full Bodies - A Voxelized Point Cloud Dataset," *ISO/IEC JTC1/SC29 Joint WG11/WG1 (MPEG/JPEG) input document WG11M40059/WG11M74006*, 2017.
- [37] Y. Xu, Y. Lu, and Z. Wen, "Owlii Dynamic human mesh sequence dataset," *ISO/IEC JTC1/SC29/WG11 m41658*, 2017.
- [38] G. Bjontegaard, "Calculation of average psnr differences between rd-curves," *VCEG-M33*, 2001.